


Building an artificial neural network with neurons

Cite as: AIP Advances 9, 075009 (2019); <https://doi.org/10.1063/1.5086873>

Submitted: 24 December 2018 . Accepted: 01 July 2019 . Published Online: 11 July 2019

M. Rigby , M. Anthonisen, X. Y. Chua, A. Kaplan, A. E. Fournier, and P. Grütter



View Online



Export Citation



CrossMark

AVS Quantum Science

Co-published with AIP Publishing



Coming Soon!

Building an artificial neural network with neurons

Cite as: AIP Advances 9, 075009 (2019); doi: 10.1063/1.5086873

Submitted: 24 December 2018 • Accepted: 1 July 2019 •

Published Online: 11 July 2019



M. Rigby,^{1,a)}  M. Anthonisen,¹ X. Y. Chua,¹ A. Kaplan,² A. E. Fournier,² and P. Grütter^{1,b)}

AFFILIATIONS

¹Physics Department, McGill University, Montreal H3A 2T8, Canada

²Montreal Neurological Institute, McGill University, Montreal H3A 2B4, Canada

^{a)}Email: matthew.rigby@mail.mcgill.ca

^{b)}Email: peter.grutter@mcgill.ca

ABSTRACT

Artificial neural networks are based on mathematical models of biological networks, but it is not clear how similar these two networks are. We have recently demonstrated that we can mechanically manipulate single neurons and create functioning synapses. Here, we build on this discovery and investigate the feasibility and time scales to build an artificial neural network with biological neurons. To achieve this, we characterized the dynamics and forces when pulling functional axonal neurites using a micromanipulation technique with maximum speeds about 300 times faster than the average natural growth rate of $0.0017\mu\text{m/s}$. We find that the maximum force required to initiate and extend the neurites is about 1nN . The dynamics of the mechanical extension of the neurite is well described by many elastic springs and viscous dashpots in series. Interestingly, we find that the transport networks, specifically the actin network, lags behind the mechanically pulled structure. These insights could potentially open a new avenue to facilitate and encourage neuronal regrowth not relying on chemical queues. The extracted mechanical parameters and timescales characterize the neurite growth. We predict that it should be possible to use a magnetic trap to wire an artificial network such as a multi-layer perceptron in 17 hours. Once wired, we believe the biological neural network could be trained to process a hand-written digit using artificial neural network concepts applied to biological systems. We show how one could test the stability and robustness of this network by axotomizing (i.e. cutting) specific axons and reconnecting them using mechanical manipulation.

© 2019 Author(s). All article content, except where otherwise noted, is licensed under a Creative Commons Attribution (CC BY) license (<http://creativecommons.org/licenses/by/4.0/>). <https://doi.org/10.1063/1.5086873>

I. INTRODUCTION

Inspired by R. Feynman's statement 'What I cannot create, I do not understand' (written on his blackboard at the time of death in February 1988), we are investigating new methods to build neuronal networks using live neurons. Artificial neural networks seem to learn in a phenomenologically similar way to the brain. The brain is extensively interconnected, estimated to have about 86 billion neurons¹ and around 100 trillion connections, it has feedback and feedforward loops² and the strength of its signal transmissions can be adjusted by adjusting the strength of its synapses.^{3,4} Similarly, artificial neural networks, which are based on mathematical models of a biological neural network, are highly interconnected, often incorporate feedback and feedforward loops and the strength of certain connections can be adjusted through backpropagation learning.⁵ Despite these similarities, the two neural networks do not process information or learn in the same way. They also differ markedly in terms of power consumption. It is not currently possible to record

all the action potentials of a biological system. For example, every neuron and every connection in the model organism *C. elegans* have been mapped, but we cannot record from every neuron in that system.⁶

In the present work, we further develop a micromanipulation technique that can be used to extend neurites from *in-vitro* axons to build a biological neural network where the topology of the network is exactly known and controlled, and all action potentials can in principle be measured. To achieve this, the neurons would be grown on a high-density multi-electrode array⁷ such that each neuron is on an electrode, while the axons would be mechanically manipulated to connect neurons. A simple artificial neural network, such as a multi-layer perceptron which could recognize hand-written digits,⁸ could be built out of neurons, and learning algorithms could be tested by stimulating neurons using the multi-electrode array. In this way, this biological neural network could be directly compared to a topologically identical artificial neural network.

Growing an interconnected biological neural network with known topology is difficult due to the limited control and speed of axonal growth: for rat hippocampal neurons grown *in-vitro*, the average elongation rate is only $0.0017\mu\text{m/s}$.⁹ By adhering to the axon and applying mechanical tension, Bray showed that neurites could be initiated out of the nucleus *de novo* and extended faster than normal growth.¹⁰ Numerous subsequent experiments by Heidemann's group showed that neurites can be characterized as viscoelastic materials exhibiting growth at speeds which are directly proportional to the applied force.¹¹⁻¹³ However, when a neurite is extended at speeds above $0.055\mu\text{m/s}$, the neurite thinned and broke.¹⁴ Growth in the central nervous system occurs through stationary periods and periods where the axonal elongation rate can be 1-2 orders of magnitude higher than the average rate,^{9,15} so an induced growth rate of $0.055\mu\text{m/s}$ is not unreasonable.

In previous experiments, we showed that by coating microbeads with a positively charged polymer (Poly-D-lysine (PDL) and netrin), an axon will form a synapse with the bead.^{16,17} By initiating the neurite from this synapse, we are able to pull at speeds of greater than $0.33\mu\text{m/s}$ over mm scale distances!^{18,19} Twelve hours after being connected to another neuron, the neurites were shown to be functionally connected using a double patch clamp measurement.¹⁸ Here, we build on these results by assuming neurites pulled by the same method would also be functional. We characterize the remarkable growth of these neurites and describe the growth using a model which consists of many springs and dashpots in series. We investigate the limits and versatility of this biophysical system with the goal of determining the parameter space for building a perceptron from real neurons. We propose a method for building a multi-layer perceptron with 496 neurons and 4215 connections with the goal of eventually building a more complex system such as *C. Elegans* with 320 neurons, 6393 chemical synapses, 890 gap junctions and 1410 neuromuscular junctions.⁶ Simpler biological circuits such as feedback or feedforward loops which require only a few neurons and electronic networks such as a 4-2-4 encoder and decoder could be similarly built using our technique to investigate the role of the diameter of the connecting axon on the transfer function of the neuronal system.

II. MATERIALS AND METHODS

A. Neuronal cultures

All neuronal cultures were approved by McGill University's Animal Care Committee (Protocol #: 2013-7422) and conformed with the Canadian Council of Animal Care Guidelines. Hippocampal neurons were dissociated as described by Lucido et al.,¹⁶ from Sprague Dawley rat embryos of either sex and plated on $100\mu\text{g/mL}$ Poly-D-Lysine (PDL) (Sigma-Aldrich) coated Mat-Tex dishes or Warner Instruments glass coverslips with neuron-specific microfluidic chambers designed by ANANDA Devices (<https://anandadevices.com/>) to ensure experiments were performed on axons. Cells were cultured for 7-21 days *in-vitro* (DIV), replacing the media every 2-3 days. On the day of the experiment, the microfluidic chambers were removed. During the experiment, media was replaced with physiological saline [135mM NaCl (Sigma-Aldrich), 3.5mM KCl (Sigma-Aldrich), 2mM CaCl₂

(Sigma-Aldrich), 1.3mM MgCl₂ (BDH), 10mM Hepes (ThermoFisher Scientific) and 20mM D-Glucose (Invitrogen)],²⁰ which was constantly replaced so that the osmolarity stayed within physiological conditions.

B. Atomic force microscopy

Atomic force microscopy experiments were conducted using either an MFP-3D-BIO AFM (Asylum Research) mounted on an Olympus IX-71 inverted optical microscope or a Bioscope-3 with Extender Module mounted on a Zeiss Axiovert s100tv. In both cases, the sample was mounted in a fluid cell, with access for the AFM cantilever, and viewed from the bottom with the optical microscope at either 40x (air) or 100x (oil immersion) Zeiss objective lenses. For force measurements, the Nanosensors qp-SCONT cantilever was used with spring constant 0.01N/m (normal force measurements) or 0.09N/m (lateral force measurements), and partial gold coating to minimize drift due to temperature changes and adsorption. Cantilevers were calibrated using the Sader method for normal and lateral spring constants.^{21,22}

C. Pipette micromanipulation

Cell media for 7-21 DIV neurons was replaced with 100nM of the live cell fluorogenic F-actin labeling probe (Si-R actin, Spirochrome) in 2mL of cell media. Immediately after, $10\mu\text{m}$ beads coated for 24 hours with $100\mu\text{g/mL}$ PDL as described previously¹⁷ were added such that the probe and the beads were incubated with the neurons for 6-9 hours. The medium containing the probe was removed along with most unattached PDL-coated beads and replaced by physiological saline solution. The neurons were imaged using a Zeiss Axiovert 200M microscope and a 63x objective (Zeiss), with the F-actin probe illuminated by a xenon arc bulb (Sutter Instruments). Pipettes (King Precision Glass) of inner and outer diameters of 1mm and 1.5mm respectively were pulled using a Sutter Instruments P-87 pipette puller to a tapered opening of between $2-6\mu\text{m}$. They were positioned using an Eppendorf InjectMan NI 2 micromanipulator, and negative suction was applied via tubing connected to a syringe. Initially a positive pressure greater than the capillary pressure was applied to generate a positive flow to avoid collection of debris on the pipette. Once the pipette opening was manipulated to be in contact with a bead adhered to a bundle of axons, a negative pressure was applied to the pipette, picking up the bead and initiating a neurite (Figure 1). The bead was manipulated vertically $\sim 3\mu\text{m}$ to avoid scraping the neurite along the surface of the dish, then it was moved at a constant velocity of $0.1-0.5\mu\text{m/s}$ parallel to the glass surface. The neurite was manipulated $100-250\mu\text{m}$, then deposited on another bundle of axons by applying positive pressure to the pipette.

D. Axotomy and reconnection

For AFM axotomy and reconnection, the Bruker MLCT-C cantilever (spring constant 0.01N/m) was used to axotomize the axon, while the Bruker MLCT-D cantilever (spring constant 0.03N/m) with PDL coated bead on the same substrate was used to reconnect the axotomized axon. For pipette axotomy and reconnection, pipettes with a flexible ending of spring constant 0.01N/m were pulled such that they could be pushed into the glass surface without

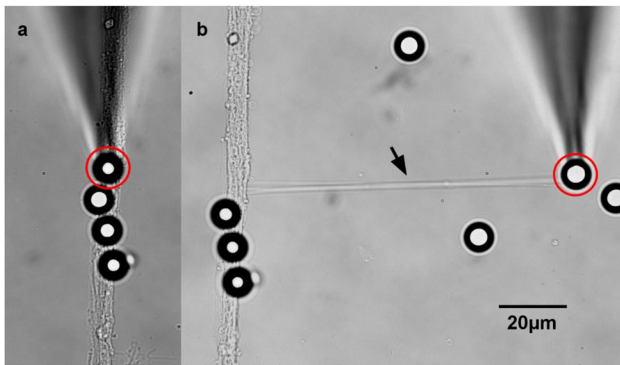


FIG. 1. (a) A pulled pipette (triangular shadow at top of image) applies suction to a PDL-coated bead (circled) and initiates a neurite by pulling upwards $\sim 3\mu\text{m}$. (b) By pulling horizontally on the bead (circled) at a constant velocity of $0.1\text{--}0.5\mu\text{m/s}$, the neurite (indicated by the arrow) is extended.

breaking. To avoid stretching the axons, the sample stage piezo was moved using a step function, moving the sample as fast as possible to make a clean cut. To test axonal fusion, a membrane impermeable dye (Alexa Fluor 488 Hydrazide) was injected at 10mM concentration in an intracellular solution as previously described¹⁸ by using a patch pipette with a $2\text{--}6\mu\text{m}$ opening and an Axon Instruments Axopatch 200A system.

E. Beading the AFM probes

1 drop of either polystyrene $10\mu\text{m}$ beads (Polysciences) or Silica $60\mu\text{m}$ beads (Microspheres-Nanospheres) was deposited on a microscope slide (Fisherbrand). The beads were dried and separated by using pressurized Nitrogen gas. Another adjacent slide was coated with E-30CL, a 2-part epoxy (Loctite). The tip was lowered to coat the underside of the cantilever with glue, then moved over to the adjacent slide to adhere the bead to the glue. Constant observation using an inverted optical microscope makes this a routine process with a high yield. For lateral AFM measurements, a $60\mu\text{m}$ and $10\mu\text{m}$ bead were glued on top of each other such that the $10\mu\text{m}$ bead contacted the axons. The $60\mu\text{m}$ bead served to increase the lever arm, reducing the cantilever torsional stiffness to 0.09N/m and to allow the measurement of the torsional deflection sensitivity. The torsional stiffness sensitivity was calibrated by laterally deflecting the cantilever on a cleaved GaAs surface glued to the surface such that the contacted surface was 90° to the horizontal.²³

F. Data acquisition and analysis

F-actin data was acquired using Northern Eclipse imaging software and a QImaging Retiga EXi camera, taking images every $4\text{--}30\text{s}$. Exposure time was 1s and gain 60% using a custom macro in the Full Control setting. The neurites were manually kept in focus for the duration of the experiment. The image stack was analyzed by drawing a line on top of the neurite and using the ImageJ Multi Kymograph plug-in v3.0.1. This produced a kymograph, which is constructed from one intensity line profile of a stack of images.

It is an image of position as a function of time, allowing the measurement of the speeds of F-actin polymers in the neurite as a function of time elapsed since pulling. These were analyzed by hand by tracing $15\text{--}30$ actin trajectories per kymograph (each kymograph was generated from one neurite). All fits were done in MatLab using lsqcurvefit to obtain the variable values and nlparci to obtain an uncertainty. Data from multiple experiments was presented as mean \pm SD. Each trajectory also gave a starting position and ending position which was converted to a starting position of actin in neurite and total movement of actin. AFM initiation curves were acquired by performing a force distance curve at $0.5\mu\text{m/s}$ using IgorPro on the Asylum MFP3D AFM system. Data acquisition rate was 1kHz , with most of the approximately $16\mu\text{m}$ dynamic range of the piezo being used. Subsequent pulls were done in the z -direction in the same way or by pulling parallel to the dish surface (in the y -direction), allowing pulls up to $50\mu\text{m}$. Pulls in the y -direction were performed using a function generator (Stanford Research Systems DS 345) by inputting a sawtooth signal into the piezo through the MFP3D Controller and pulling at $0.5\mu\text{m/s}$. The cantilever signal was acquired at 10kHz acquisition rate through MatLab which was connected to a National Instruments data acquisition card with 4096 pixel resolution.

III. RESULTS AND DISCUSSION

A. Building a neural network from neurons

A simple artificial neural network for image recognition of the hand-written numbers $0\text{--}9$ consists of 16×16 inputs,²⁴ 2 deep layers of 15 neurons each and 10 outputs.⁸ The same configuration of neurons was then chosen as shown in Figure 2 to get an estimate of how long it would take to build a neuronal network from neurons. In a perceptron, every neuron from a previous layer is connected to every neuron from the next layer. This means that the total manipulation distance for the setup proposed would be given by:

$$d = s \sum_{i,j,k} \sqrt{(n+1-i)^2 + (j-k-1)^2} + s \sum_{j,k} \sqrt{1+(j-k)^2} + s \sum_{j,k} \sqrt{1+(j-k-2)^2} \quad (1)$$

Where the variable i represents the indices for the rows, j and k represent the indices for subsequent layers of columns in Figure 2 and n is the total number of rows in the first layer. The first term in equation (1) corresponds to the total amount of neurite needed to be manipulated to connect every neuron from the layer of input neurons to the first deep layer of neurons. Similarly, the second and third terms in the equation correspond to the two remaining layers being connected. The reason we sum over i , j and k in the first term, but only j and k in the second terms is that the first layer of input neurons has multiple rows (n rows) whereas the others only have one row. On a high-density multi-electrode array, separating the neurons by $s=30\mu\text{m}$ would allow recording from each neuron. This means that the total manipulation distance for the requisite 4215 connections is 1.288 meters. In the following we will investigate if this is theoretically feasible using mechanical pulling of neurons.

From a bio-engineering perspective, there is no reason to choose this task and neural network over another. However, the

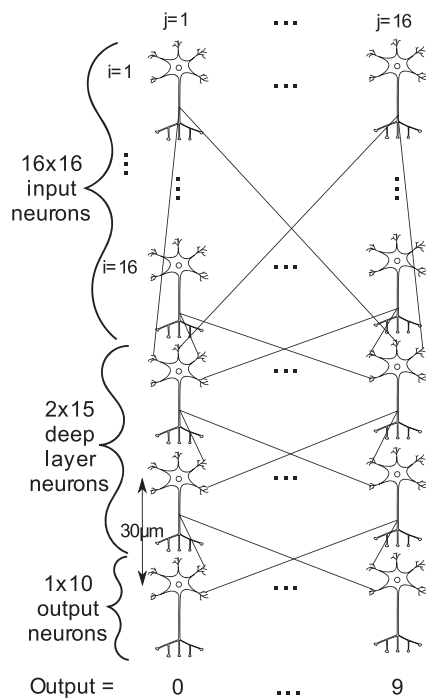


FIG. 2. Multilayer Perceptron: Each neuron from the 16x16 block of input neurons will connect with each neuron from the first deep layer of 15 neurons. This is true for all adjacent layers (i.e. all neurons in one layer are connected to all neurons in the next layer).

identification of hand-written digits has been extensively studied in the machine learning community, and deep learning techniques have been very successful at performing this task. This has led to it being called “the drosophila of machine learning” by Geoffrey Hinton,⁵ so it makes a simple, but good candidate for making an artificial neural network from a biological one. We do not intend on building this network ourselves but would simply like to show that it is possible to build a neural network from neurons which can solve a real task.

B. Force requirements

In order to wire a neural network, the manipulation method must be able to exert a large enough force to initiate and extend the neurites. Using an atomic force microscope to measure mechanical properties,²⁵ we found that the force required to initiate and extend a neurite varies significantly. To initiate a neurite, the maximum force was $1.1 \pm 0.7 \text{ nN}$ (Figure 3a) and to continue extending the neurite, the average force was $1.1 \pm 0.8 \text{ nN}$ (Figure 3b) for 5 different experiments at pulling speed $0.5 \mu\text{m/s}$. The large variability in the force needed is likely due to the variation in number of neurites being pulled. For these experiments, we often initiated neurites from bundles of neurons, possibly initiating the pulling of several neurites. The values quoted above are thus the maximum forces needed to initiate pulling of single neurites because the maximum force to initiate and pull one neurite will be less than or equal to the force obtained when pulling multiple neurites.

During the initiation of a neurite, the force does not simply increase with stretch as in Hooke’s law.²⁶ The force initially increases very quickly, followed by a decrease in force, then finally after much more extension, the force begins to increase gradually again. According to both Powers et al.,²⁷ and Derenyi et al.,²⁸ the bead initially pulls out a portion of the axon into a catenoid as shown in Figure 4. However, the boundary conditions of a catenoid are only stable when the neurite is below a specific length such that the neurite starts to collapse into a thin tube beyond this length and the force decreases.^{27,28} As the pull continues, the tube starts to stretch, and the force increases again.²⁹ Over the first $10 \mu\text{m}$,³⁰ this increase is approximately linear, but is clearly viscoelastic on longer length scales (Figure 3b). The simplest model that exhibits both viscous and elastic behavior is the Maxwell viscoelastic body and consists of a dashpot with viscosity μ and a spring with stiffness constant k . The force F as a function of extension x for a neurite being pulled at a constant velocity v is then:^{31,32}

$$F(x) = \mu v \left(1 - e^{-\frac{k}{\mu v} x} \right) \quad (2)$$

The spring constant and viscosity obtained from fits as in Figure 3b from 5 different neurites is $56 \pm 35 \mu\text{N/m}$ and $2.8 \pm 2.2 \text{ mNs/m}$ respectively. The significant variation in these values is again likely due to the variation of the number or diameter of neurites initiated.

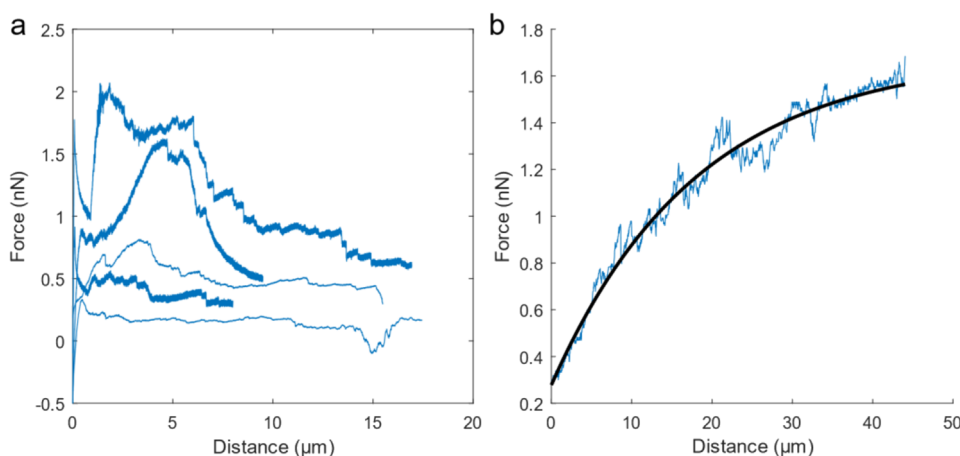


FIG. 3. (a) Initiation of Neurites from 5 different experiments (maximum forces are $F=1.98 \text{ nN}$, 1.60 nN , 0.81 nN , 0.85 nN , 0.24 nN). (b) Following initiation, the neurite is elongated, and the force is fit with a Maxwell viscoelastic model.

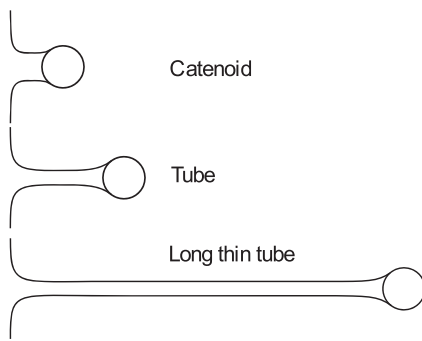


FIG. 4. The neurite is initially a catenoid until the boundary conditions become unstable, and it collapses into a tube. The tube stretches with elongation but maintains the same approximately cylindrical shape.

C. Pulling speeds

Using our micromanipulation technique, we can pull at a remarkably fast $0.5\mu\text{m/s}$ to wire any two neurons together. Previous work has been done to show that the neurite is functional after 24 hours. The neurite contains actin, tubulin and neurofilament and it has been shown to be electrically connected to another neuron.¹⁸ As far as we can determine, these ‘pulled’ neurons are structurally and functionally not distinguishable from naturally grown ones. An intriguing question is why is it possible to pull so fast? Is the neurite growing at this speed or is the plasma membrane stretched and the neurite subsequently filled with cytoskeletal elements? These are biologically interesting questions that are important to understand the limits to how fast we can build a complex neuronal network.

To answer this question, we fluorescently labelled F-actin, an important cytoskeletal element, and used it as a proxy for growth leading to biologically relevant structure and functionality. After stretching/extending the neurite hundreds of micrometers at $0.1\text{--}0.5\mu\text{m/s}$, the neurite is held at a constant length, and the maturation of the neurite can be observed. Immediately after stopping the extension, actin appears to be pulled into the neurite. This can be seen in the kymograph in Figure 5a.

As in section III B, we can model the actin in the neurite as a Maxwell material, but this time with many Maxwell elements in series³² (the exact details for the model are given in section III E). We thus derived the position of the i^{th} element of F-actin cytoskeleton in the neurite as a function of time to be:

$$d_i(t) = A \left(1 - e^{-\frac{t}{\tau}} \right) \quad (3)$$

Where A is the displacement of the actin and τ is the characteristic time it takes for the actin to arrive to its final position in the neurite. We fit equation (3) to the data in Figure 5b, and we see that the characteristic time τ is a constant independent of the actin position in the neurite (Figure 5c). Since τ is a constant throughout the neurite, we can use the average τ to determine the growth rate of the whole neurite. The average τ for all the actin movement in a neurite, measured in 7 different experiments, is $15.5 \pm 9\text{min}$. Using actin cytoskeleton as a proxy for growth, where the growth is assumed to be finished after $t = 3\tau$ (when the distance the actin travelled is 95% of the total distance the actin will travel), these values translate to an effective

growth rate of $0.048 \pm 0.02\mu\text{m/s}$. This is calculated by dividing the total length of the neurite by 3τ plus the pull time. The maximum growth rate achieved without neurite thinning and breaking for Fass et al.,¹⁴ was $0.055\mu\text{m/s}$, indicating that the actual biological growth speed in our experiments is similar to the growth rates seen by others.¹⁴ In their experiments however, they were not able to pull faster without the neurite breaking.

There are two main differences between the initiation of neurites in our experiments and those by others.^{11–14} The first is that we initiate the neurites *de novo* from axons whereas normally neurites are initiated *de novo* from the cell body. The second is that our axon forms a pre-synapse with the bead before initiation whereas we do not believe that is the case in other experiments. We believe that others initiate neurites using simple adhesion because they all initiate their neurites from the cell body, whereas pre-synapses are formed on axons. In addition to this, it takes at least 30 minutes to form a synapse with a PDL-coated bead.¹⁶ Bray left the polylysine coated pipette in contact only “10 minutes or so”,¹⁰ Heidemann’s group initiate neurites immediately after coming in contact with the cell,^{11–13} and the Integrin-coated beads added to the cells by Fass et al.,¹⁴ were added once the neurons were in the manipulation setup, meaning they were not in contact long before the neurites were initiated (the exact time was not specified).¹⁴ Heidemann’s group also frequently pulls the growth cone of already formed axons, however, the fact that the axon is adhered to the surface slows the growth rate down because the adhesion increases its viscosity.³³ In our experiments, the neurite is always suspended in the solution, so we do not have this issue. It is possible that, in our experiments, the presence of an already formed axon adjacent to the neurite with a strong connection in the form of a synapse is better able to provide cytoskeleton and plasma membrane than a cell nucleus on its own, allowing for quicker pulling and the generation of a ‘guiding structure’ which later fills with the cytoskeletal components present in all axons.

D. Network robustness

Once the neural network has been trained using images provided openly in the NIST database,²⁴ we would be able to determine the contribution of each neuron and its connections to the success of the network. To test this experimentally, we could sever individual axons (axotomy) and then reconnect them. In Figure 6, we axotomized an axon using an atomic force microscope (AFM) cantilever, then used a PDL-coated bead glued to another AFM cantilever to micromanipulate one axotomized end into contact with the other. Subsequent experiments were encouraging but inconclusive as to whether the two axotomized ends fused. The newly grown neurites did show transport in both the proximal and distal ends, but it is unclear whether there is transport across the reconnection.

In further experiments designed to see if fusion between the two axotomized ends of the axon can occur simply by pressing the two ends together, we used patch clamp to input a membrane impermeable dye into the nucleus following axotomy and reconnection. In one experiment, the dye was found in the distal end of the neurite. This appears to show fusion, but we only observed it once. There are a few reasons why fusion may not be observed: the axon forms a synapse with the bead (so wouldn’t fuse with the distal part

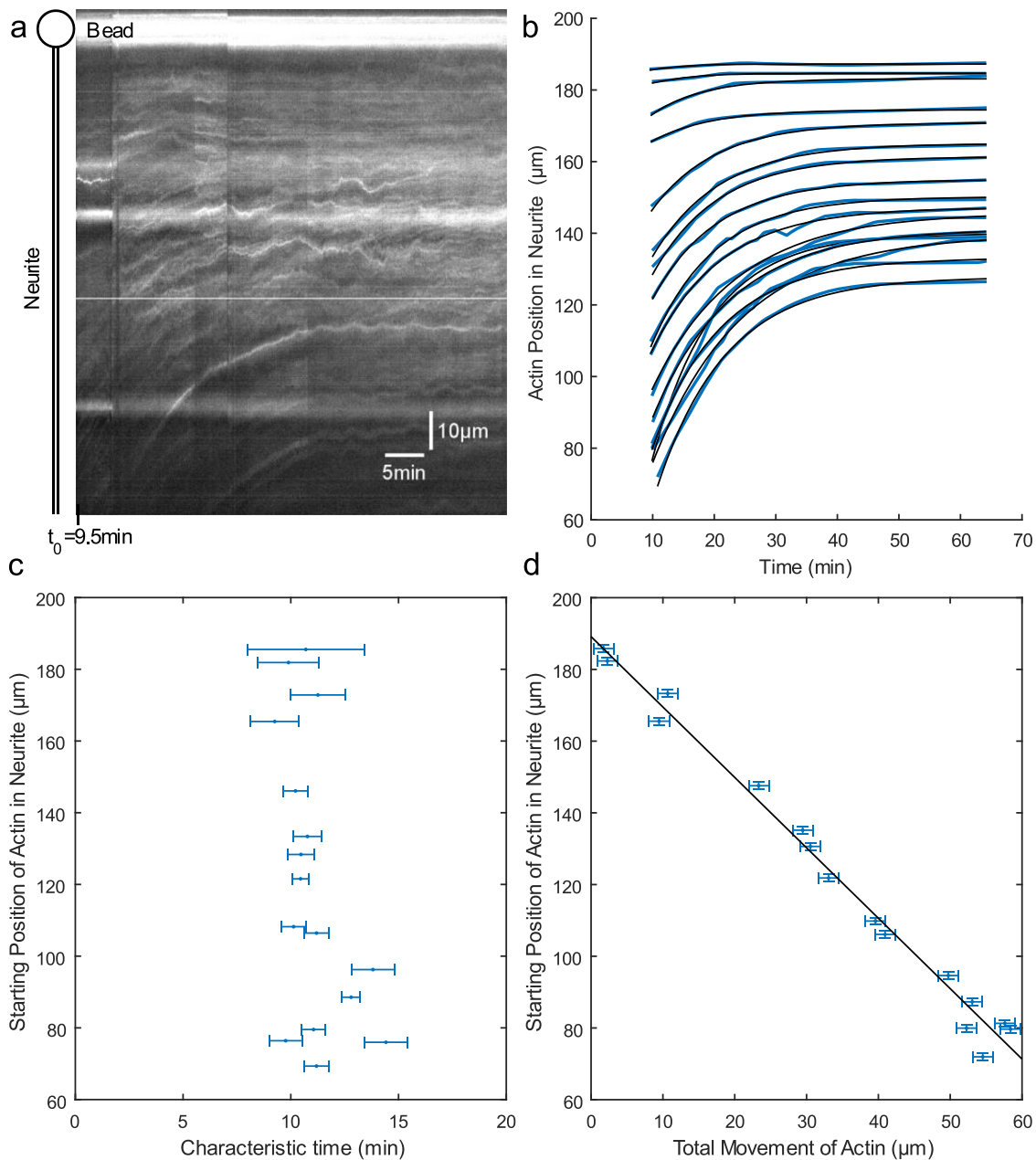


FIG. 5. Movement of actin in the neurite after extension: (a) Kymograph of the actin starting 9.5min after extending neurite. The bead is at the top of the image, and the neurite extends straight down as in the drawing on the left. (b) Traces of actin from the kymograph in (a) with equation (4) fit to the data. (c) The characteristic time τ , a fit parameter in equation (4), is independent of the starting position of actin in the neurite. The characteristic time is equal to the spring constant divided by the viscosity of the neurite. (d) The total movement of actin has an inverse linear dependence on the starting position of actin in the neurite.

of the axon), the cell would sometimes undergo Wallerian degeneration following axotomy, finding the correct nucleus to patch to experimentally demonstrate successful fusion was difficult as there were many axons taking similar paths, and it is possible that the fusion does not occur every time. The fact that we did not observe routine fusion following axotomy is unsurprising due to the above

mentioned challenges. Furthermore, it has also not been observed in mammalian axons to our knowledge (except by using methods which break down the membrane structure).³⁴ It has been observed to occur by axonal regeneration in *C. elegans*, crayfish, earthworm and leech.³⁵ Irrespective of whether the proximal and distal ends of the severed neuron can fuse using our micromanipulation technique

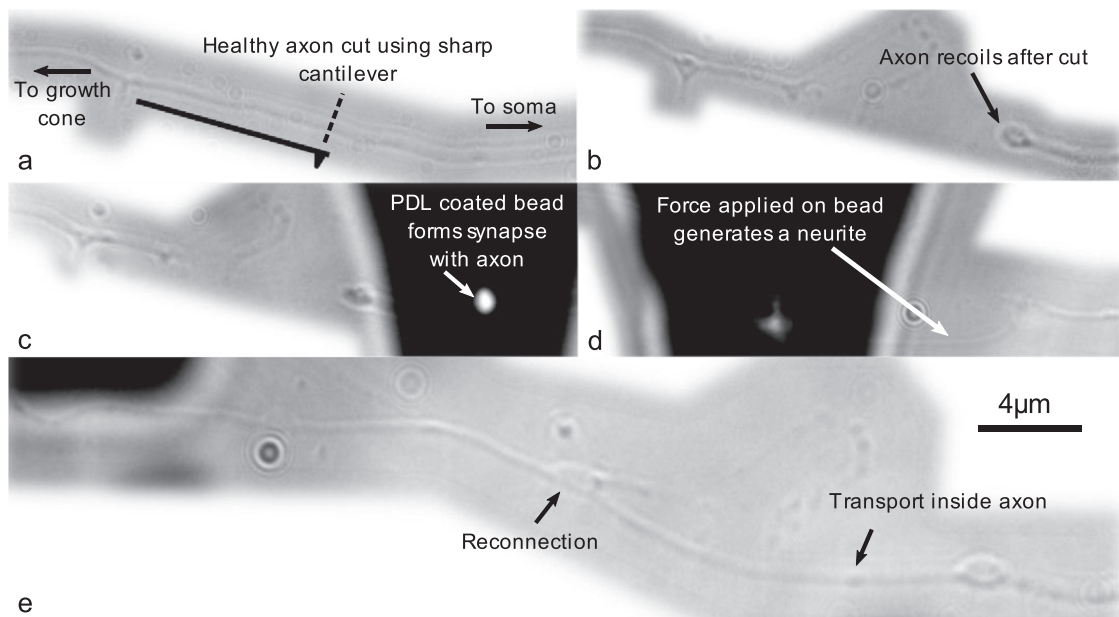


FIG. 6. Axotomy and Reconnection. (a) A single healthy axon is cut along the dash line using a sharp cantilever. (b) Axon following axotomy. (c) A PDL-coated bead glued to bottom of cantilever (large black object) forms a synapse with proximal end of the axotomized axon. (d) Force applied by cantilever and bead on axon generates a new neurite. (e) Neurite reconnects the axon's proximal and distal ends. The axon appears to be reconnected and has transport in the proximal end, but not definitively in the distal end.

and by pressing the two ends together, it has been routinely shown that the two ends can be fused by using a technique called microelectrofusion.^{34,36} This method works by dissolving the membrane using high electric pulses such that the membrane fuses into a single tube when it re-solidifies. We have showed here that by using microelectrofusion and our micromanipulation technique, we can systematically study the role of individual connections in the neural network.

E. Model of the mechanical properties of the neurite

In sections III B and III C, we used a Maxwell viscoelastic model (Figure 7b) to fit force data and actin movement data respectively. In the constant velocity extension curves in Figure 3b, the force increases, indicating stretch. This provides the motivation for the elastic component in the Maxwell model. The viscous component allows viscous flow to relax the spring, shown by the force plateau in Figure 3b. Solving for the force as a function of extension at constant speed gives equation (2) which was used to fit the data in Figure 3b. Since the neurite is well modeled as a spring and dashpot in series, it seems reasonable to model the transport of actin along the length of the neurite similarly. One spring and dashpot in series is mathematically equivalent to many connected smaller Maxwell elements. Since we are examining the actin movement throughout the length of the neurite, we propose a viscoelastic model consisting of many Maxwell elements in series³² and derive the displacement of each element as a function of time (the model in Figure 7a shows only the springs to make the visualization of each spring's displacement easier to follow).

The flow of actin into the neurite occurs after the neurite is extended and the springs are stretched out (Figure 7a). The tension from the stretching pulls more material into the neurite by overcoming the viscous resistance, relieving tension and effectively elongating the neurite. Each spring in the neurite will feel the same force and will be stretched equally because the springs are arranged in series. In Figures 7a and 5c, we see that the total displacement d_i of the proximal springs (those closest to the axon-neurite junction) will be much larger than the displacement of the distal springs (those closest to the bead). This is because the full displacement of the i^{th}

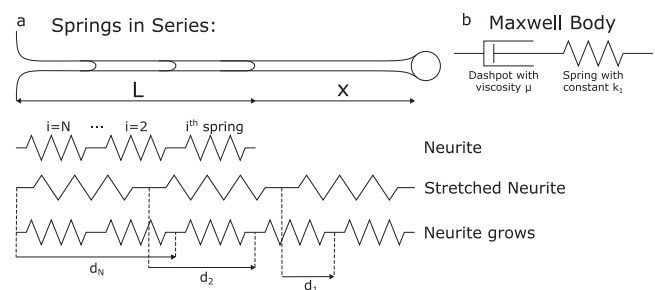


FIG. 7. Physical model of the neurite during extension: (a) When modelling the neurite as many springs (and dashpots, not shown) in series, we can predict where each spring will be relative to each other in the neurite by calculating d_i as a function of d_{i-1} . (b) Maxwell viscoelastic body: the movement of the actin in time cannot be instantaneous because there is viscous flow. We model this by putting a dashpot in series with each spring in the neurite.

spring is equal to the total amount of stretch of all the springs in front of it:

$$d_i(t) = \frac{i}{N}x - ix_i(t) \quad (4)$$

Here, N is the total number of springs in the neurite, x is the total amount of initial stretch in the neurite, and x_i is the instantaneous stretch in each spring. Each elastic spring element is accompanied by a viscous element (modelled by a dashpot) to represent the resistance of the neurite to flow. Each spring and dashpot will experience the same amount of force, so that we can write the force applied on each element in the neurite as:

$$F_i = k_s x_i = \mu_d (\dot{d}_i - \dot{d}_{i-1}) \quad (5)$$

We have assumed that the spring constant k_s and the viscosity μ_d of all constituents are the same, which agrees with the linear trend in Figure 5d. Combining equations (4) and (5), and solving the resultant differential equation gives:

$$d_i(t) = \frac{ix}{N} \left(1 - e^{-\frac{k_s}{\mu_d} t} \right) \quad (6)$$

Which describes the displacement of the i^{th} element of the neurite as a function of time. Equation (3) is the same as equation (3), only we have now defined $A = ix/N$ and $\tau = \mu_d/k_s$. As noted in section III C, the characteristic time $\tau = \mu_d/k_s$ is a constant independent of the actin position in the neurite (Figure 5c). This indicates that the tension is distributed equally throughout the neurite, allowing all constituents to relax together, and providing evidence there is a similar composition along the length of the neurite. The neurite displays a remarkable ability to stretch itself, with the actin pulled mechanically into the neurite.

Equation (6) also indicates that the total movement of actin in the neurite should be smaller for actin that starts distally and that this should have a linear dependence. This is what we observe in Figure 5d. The deviation of this line from the $y = -x$ line is the total length of springs in the neurite measured in equilibrium, $L = Nl$, where l is the length of one unstretched spring. In terms of variables defined in the model, Figure 5d is a plot of $ix_i + L$ vs $(i/N)x$. As we would expect, neurites which were pulled a longer distance had both a longer length L and initial stretch x (data not shown).

The model describes all aspects of the data, providing evidence that the flow of actin is mechanically driven by the force applied to the neurite. The neurite does not grow at the pulling rate set by the user, but instead stretches, and later fills in with a characteristic time which depends on the spring constant and the viscous resistance. When compared to other mechanically induced growth in neurites, the effective growth rate of these neurites is similar. However, because we are able to pull much faster, this allows the possibility to wire a complex neural network in a comparatively small amount of time.

F. Optimal manipulation

With our micromanipulation technique, we can pull at $0.5\mu\text{m/s}$, meaning it would take 30 days of pulling time to wire the proposed multilayer perceptron network's 1.288 meters total length. This is prohibitively slow: The cells will die well before the 30 days of manipulations are complete, as the manipulation is not performed in an incubator with optimal conditions for neuron survival. A more

realistic maximum time for completing these manipulations before the cells die is empirically about 24 hours; an effective speed up of about 30 times is thus necessary. The only solution to reduce the manipulation time by this much would be to pull multiple beads simultaneously.

The necessary criteria for wiring an arbitrary neural network are:

1. The setup must keep cells alive for many hours.
2. It must be possible to manipulate in all 3 dimensions.
3. Most importantly, as described in section III B, the method must be able to exert a large enough force to initiate and extend the neurites.

There are many techniques for manipulating microspheres in a dish. Optical tweezers can be multiplexed, but the trap force maximum is generally about 100pN and the laser can cause photodamage and heat the sample significantly, both leading to cell death.³⁷ Acoustic force spectroscopy and centrifugal force spectroscopy both lack multidimensional motion.^{38,39} An atomic force microscope cantilever array has many positives, but it cannot effectively release the beads as these are usually glued to the end of the cantilevers.⁴⁰ By making a hole in the bottom of the cantilevers, it could be possible to use suction to pick up the beads, but this method still lacks independent control over each bead.⁴¹ Magnetic traps have been multiplexed by positioning a magnet far away from the beads, such that all beads feel the same field. However, the multiplexing abilities mean that the magnets are positioned quite far away such that the maximum force is 260pN, and in most systems significantly less.^{42,43} The multiplexed traps also lack independent control as they exert the same force on all beads.

The best option seems to be to use 2-3 magnetic pole pieces similarly to Fass et al.,¹⁴. Since the pole pieces are mounted on a micromanipulator, each pole piece would give control over another dimension, the pole pieces can be brought into proximity with the magnetic bead of choice (allowing a large range of force control and bead selectivity) and this method does not kill the cells. Using an electromagnet, the force dependence on distance is a power law⁴⁴ which allows manipulating specific beads based on proximity to the pole pieces. Also, the force depends linearly on the current flowing through the solenoid⁴⁴ allowing quick adjustments to the force applied. Using a $4.5\mu\text{m}$ bead, and by varying the distance and the current, it is possible to apply forces that range from 15pN up to many nanonewtons.¹⁴

This method could be multiplexed by picking up each bead in a column (see Figure 2) in one pass, such that many beads will all be pulled together. An appropriate field gradient could be one where a bead $14\mu\text{m}$ away would feel a force of around 1nN, sufficient to initiate and extend a neurite. Using this field, a bead on an adjacent axon another $30\mu\text{m}$ away (and thus a total of $44\mu\text{m}$ away), would feel only 0.1nN force, so it would not be initiated. For reference, a bead 10, 20, 30, 40 and $50\mu\text{m}$ away from the pole piece would feel a force of 2.0, 0.5, 0.22, 0.12 and 0.078nN respectively. In the situation where a bead on an adjacent axon was for example only $20\mu\text{m}$ away, it could be inadvertently initiated. This should be avoidable though because each bead is placed on the axon by the user and the multi-electrode arrays are separated by $30\mu\text{m}$ (although some optimization might be necessary here). Using these parameters, many beads could

be picked up sequentially and connected to their common destinations simultaneously. Each pass would thus connect one column of 16 neurons in the first layer to every neuron in the entire row of 15 neurons in the next layer.

Since the input neurons form a 16x16 square of neurons, each column of this square could be pulled at one time simply by picking up a bead and moving on to the next row of neurons to pick up the next bead and initiate another neurite. To connect these newly initiated neurites to the dendrites of the next layer's neurons, the neurites could be connected by wedging them under a non-magnetic bead sitting on the target neuron's dendrites. In this way, the column of neurons will have their neurites connected to each neuron's dendrites in the next layer's row in one single pass. This would reduce the amount of pulling time from about 42 days in sequential pulling, as calculated at the beginning of this section, to about 10.3 hours. Of course, for this to work, 296 beads would have to be precisely placed on the axons and dendrites throughout the dish. Placing a bead takes about 1 minute, so this would add about 5 more hours. Adding another hour for the user to operate the setup and make decisions in real time implies that it should be possible to wire the entire circuit in only 17 hours. Based on these considerations, using multiple magnetic pole pieces to connect this circuit seems feasible.

G. A learning biological neural network

Once the neural network has been successfully wired, the connections will be initially firing randomly, and will not be able to process a hand-written digit. In an artificial neural network, teaching a neural network to recognize a digit is done through a method called backpropagation. Each input neuron receives a pixel value from 0 to 1 from the initial 16x16 image, and the signal is passed through the layers to the output layer. As the signal passes from one layer to the next, the activation energy (neuron initial value), the weight (factor multiplied with the activation energy) and the bias (offset added at the end) will be scaled to determine what value between 0 and 1 the next neuron will take.⁸ Teaching the network adjusts those three variables for every connection in the network appropriately to maximize the chance of outputting the correct number. Backpropagation works by calculating the cost function (the sum of the difference between the output and the input), and figures out what values of activation energies, weights and biases will give the correct value. This is done by minimizing the gradient of the cost function on a large set of training data.

In a biological neural network, Hebbian theory says that neurons can adjust the strength of their connections by increasing the number of synaptic connections or by changing the nature of their synapse (e.g. by increasing synaptic vesicle exocytosis) in a process called long-term potentiation.^{45,46} Long-term potentiation is analogous to increasing the weight of a connection in an artificial neural network. Pre- and post-synaptic neurons depolarizing together during a high frequency stimulation can cause long-term potentiation.⁴ Certain pathways may be inadvertently strengthened, but with the multi-electrode array, those pathways can be discouraged by hyperpolarizing select cells, preventing them from being strengthened. Bienenstock, Cooper and Munro (BCM) developed a theory which builds on Hebbian theory and says that when a pre-synaptic

neuron is stimulated, but the post-synaptic activity is below a certain threshold, long-term depression will occur.⁴⁷ Long-term depression is the functional opposite of long-term potentiation and is analogous to decreasing the weight of specific connections. By inducing either long-term potentiation or depression, specific connections can be either encouraged or discouraged.^{4,48,49} Synaptic plasticity can be induced using other methods such as: the pairing of depotentiation in pre- and post-synaptic neurons,⁵⁰ using naturally occurring firing patterns to induce LTP,⁵¹ or by using N-methyl-D-aspartate to induce LDP.⁴⁹ Non-synaptic forms of plasticity which affect all the synapses in a cell⁵² or membrane geometric properties⁵³ also exist.

A significant difference between a neuron and a computer is that a neuron will only fire if it reaches a threshold polarization, and its strength of polarization is always the same, which means that the analog of activation energy in an artificial neural network is not the same as changing the strength of the action potential in a biological neural network. Instead, information is encoded through stimulation pulses.⁵⁴ We could make high frequency pulses in a biological neural network analogous to higher activation energies in an artificial neural network. The pixel values that were encoded in the artificial neural network with a value between 0 and 1 could instead be encoded using higher and lower frequency inputs. Since the multi-electrode array allows both the stimulation and recording of action potentials of all the neurons in the dish, the entire network could be analyzed with the gradient of the cost function as in an artificial neural network. By systematically changing the long-term potentiation and depression of specific connections, the network could then be trained using backpropagation.

Assuming an artificial neural network with the exact topography described in section III A is successfully built, there will still be a number of challenges in the actual training of the neural network and the interpretation of its outputs. These are challenges present in any artificial neural network, but with the added complexity that the network is slower to train, the activation energy here is encoded as a frequency and the neuron may compute information in a fundamentally different way.

The biggest challenge would be if the biological neural network is unable to learn at all and the error rate on the training dataset never decreases significantly (underfitting). The strength of the connections between neurons are altered by inducing physiological changes to each connection, meaning that the neurons will take much longer to train than an artificial neural network. This means that it may not be possible to do more than 1 epoch (i.e. one pass through the entire training dataset, which for the MNIST dataset is 60000 hand-written digits), and hence the data will be underfit.⁵ To compensate for this limitation, it may be more efficient to increase the number of training examples between each change to connection strengths. Another reason the network is underfitting could be due to fundamentally different computational methods between an artificial neural network and a biological one (e.g. because the frequency of the signal may not encode the activation energies properly). We know there are differences in how the two networks compute, and this may necessitate a different approach for training the network. Rather than specifying the exact algorithm for computing to the network, letting it figure out how to best process the information itself might give insights into how a biological neural network naturally

computes. However, this will be difficult as we do not yet have a clear idea of how the network computes, so it will be difficult to know how to train the network (i.e. what behavior to encourage or discourage).

The opposite scenario where the network performs well on training data but does not perform well on test data is called overfitting. In this case, the capacity of the network will need to be reduced. In an artificial neural network, one way this is done is by using different types of non-linear functions for calculating the activation energies.⁵ However, for a biological neural network, the neuron fires if depolarized below a certain threshold and this is intrinsic to the neuron, so it is not possible to change this. Instead, other techniques for reducing the capacity of the network should be employed, such as reducing the number of neurons in the deep layers or reducing the number of epochs. Following these adjustments, if the network can successfully classify the hand-written digits from the test dataset (10000 digits), then we can be satisfied that the network has truly learned how to perform a complex task. We believe that the process of getting to this point will be important in understanding the difference between the biological neural network and the artificial one.

IV. CONCLUSION

We believe that building an artificial neural network from biological neurons will help to understand what is fundamentally different between a brain and a machine. We propose a method to train the network by using backpropagation, which is used on artificial neural networks, by systematically changing the weight of the connections between neurons and by using frequencies to encode what would normally be entered as the activation energies of an artificial neural network. We propose using a multi-electrode array, to record all action potentials and stimulate any neuron, which would allow us to measure and systematically change any of the weights of the connections between neurons, capabilities which are not currently available for any complex network. The bioengineering feat of wiring all the connections into a complex biological neural can be done by using our micromanipulation technique which can pull 300 times faster than average natural growth. We have shown that the maximum forces required to initiate and elongate these neurites is within the capabilities of a magnetic trap. We have developed a model which describes the remarkable mechanically induced growth in the neurite. Furthermore, we have shown that it could be possible to test the robustness of this network by axotomizing specific axons and then reconnecting them. We believe that all the necessary knowledge and technology is available to build and teach an artificial neural network from biological neurons which will allow new insights into computation and learning in both machines and in brains.

ACKNOWLEDGMENTS

Funding from McGill University, NSERC, FRQNT and CIHR are gratefully acknowledged. The authors would like to thank everyone in the Grütter lab and the Fournier lab for useful discussions, especially Yoichi Miyahara whose technical expertise in the lab has been an enormous help.

REFERENCES

- ¹F. A. C. Azevedo, L. R. B. Carvalho, L. T. Grinberg, J. M. Farfel, R. E. L. Ferretti, R. E. P. Leite, W. J. Filho, R. Lent, and S. Herculano-Houzel, *J. Comp. Neurol.* **513**, 532 (2009).
- ²A. Longstaff, in 3rd ed. (Taylor & Francis, 2011).
- ³H. Pinsky, I. Kupfermann, V. Castellucci, and E. Kandel, *Science* **167**, 1740 (1970).
- ⁴T. V. Bliss and T. Lomo, *J. Physiol.* **232**, 331 (1973).
- ⁵I. Goodfellow, Y. Bengio, and A. Courville, *Deep Learning* (MIT Press, 2016).
- ⁶L. R. Varshney, B. L. Chen, E. Paniagua, D. H. Hall, and D. B. Chklovskii, *PLOS Comput. Biol.* **7**, e1001066 (2011).
- ⁷D. Jäckel, D. J. Bakum, T. L. Russell, J. Müller, M. Radivojevic, U. Frey, F. Franke, and A. Hierlemann, *Sci. Rep.* **7**, 978 (2017).
- ⁸M. A. Nielsen (2015).
- ⁹C. G. Dotti, C. A. Sullivan, and G. A. Banker, *The Establishment of Polarity by Hippocampal Neurons in Culture* (1988).
- ¹⁰D. Bray, *Dev. Biol.* **102**, 379 (1984).
- ¹¹T. J. Dennerll, P. Lamoureux, R. E. Buxbaum, and S. R. Heidemann, *J. Cell Biol.* **109**, 3073 (1989).
- ¹²J. Zheng, P. Lamoureux, V. Santiago, T. Dennerll, R. E. Buxbaum, and S. R. Heidemann, *J. Neurosci.* **11**, 1117 (1991).
- ¹³S. Chada, P. Lamoureux, R. E. Buxbaum, and S. R. Heidemann, *J. Cell Sci.* **110**, 1179 (1997).
- ¹⁴J. N. Fass and D. J. Odde, *Biophys. J.* **85**, 623 (2003).
- ¹⁵G. Ruthel and G. Banker, *J. Neurobiol.* **39**, 97 (1999).
- ¹⁶A. L. Lucido, F. Suarez Sanchez, P. Thstrup, A. V. Kwiatkowski, S. Leal-Ortiz, G. Gopalakrishnan, D. Liazoghli, W. Belkaid, R. B. Lennox, P. Grutter, C. C. Garner, and D. R. Colman, *J. Neurosci.* **29**, 12449 (2009).
- ¹⁷J. S. Goldman, M. A. Ashour, M. H. Magdesian, N. X. Tritsch, S. N. Harris, N. Christofi, R. Chemali, Y. E. Stern, G. Thompson-Steckel, P. Gris, S. D. Glasgow, P. Grutter, J.-F. Bouchard, E. S. Ruthazer, D. Stellwagen, and T. E. Kennedy, *J. Neurosci.* **33**, 17278 (2013).
- ¹⁸M. H. Magdesian, G. M. Lopez-Ayon, M. Mori, D. Boudreau, A. Goulet-Hanssens, R. Sanz, Y. Miyahara, C. J. Barrett, A. E. Fournier, Y. De Koninck, and P. Grutter, *J. Neurosci.* **36**, 979 (2016).
- ¹⁹M. H. Magdesian, M. Anthonisen, G. M. Lopez-Ayon, X. Y. Chua, M. Rigby, and P. Grütter, *J. Visualized Exp.* e55697 (2017).
- ²⁰J. S. Goldman, M. A. Ashour, M. H. Magdesian, N. X. Tritsch, S. N. Harris, N. Christofi, R. Chemali, Y. E. Stern, G. Thompson-Steckel, P. Gris, S. D. Glasgow, P. Grutter, J.-F. Bouchard, E. S. Ruthazer, D. Stellwagen, and T. E. Kennedy, *J. Neurosci.* **33**, 17278 (2013).
- ²¹J. E. Sader, J. W. M. Chon, and P. Mulvaney, *Rev. Sci. Instrum.* **70**, 3967 (1999).
- ²²C. P. Green, H. Lioe, J. P. Cleveland, R. Proksch, P. Mulvaney, and J. E. Sader (2004).
- ²³R. J. Cannara, M. Eglin, and R. W. Carpick, *Rev. Sci. Instrum.* **77**, 053701 (2006).
- ²⁴Y. Lecun, L. Bottou, Y. Bengio, and P. Haffner, *Proc. IEEE* **86**, 2278 (1998).
- ²⁵Y. F. Dufrène, T. Ando, R. Garcia, D. Alsteens, D. Martinez-Martin, A. Engel, C. Gerber, and D. J. Müller, *Nat. Nanotechnol.* **12**, 295 (2017).
- ²⁶R. Hooke, *Lectures de Potentia Restitutiva, or Of Spring* (1678).
- ²⁷T. R. Powers, G. Huber, and R. E. Goldstein, *Phys. Rev. E* **65**, 041901 (2002).
- ²⁸I. Derényi, F. Jülicher, and J. Prost, *Phys. Rev. Lett.* **88**, 238101 (2002).
- ²⁹O. Rossier, D. Cuvelier, N. Borghi, P. H. Puech, I. Derényi, A. Buguin, P. Nassoy, and F. Brochard-Wyart, *Langmuir* **19**, 575 (2003).
- ³⁰M. Anthonisen, M. Rigby, M. H. Sangji, X. Y. Chua, and P. Grütter, *J. Mech. Behav. Biomed. Mater.* **98**, 121 (2019).
- ³¹J. Schmitz, M. Benoit, and K. E. Gottschalk, *Biophys. J.* **95**, 1448 (2008).
- ³²W. Findley, J. Lai, and K. Onaran **19**, 118 (1978).
- ³³P. Lamoureux, S. R. Heidemann, N. R. Martzke, and K. E. Miller, *Dev. Neurobiol.* **70**, 135 (2010).
- ³⁴W. C. Chang, E. Hawkes, C. G. Keller, and D. W. Sretavan, *Wiley Interdiscip. Rev. Nanomedicine Nanobiotechnology* **2**, 151 (2010).

- ³⁵B. Neumann, K. C. Q. Nguyen, D. H. Hall, A. Ben-Yakar, and M. A. Hilliard, *Dev. Dyn.* **240**, 1365 (2011).
- ³⁶G. A. Neil and U. Zimmermann, *Methods Enzymol.* **220**, 174 (1993).
- ³⁷K. C. Neuman and A. Nagy, *Nat. Methods* **5**, 491 (2008).
- ³⁸G. Sitters, D. Kamsma, G. Thalhammer, M. Ritsch-Martel, E. J. G. Peterman, and G. J. L. Wuite, *Nat. Methods* **12**, 47 (2015).
- ³⁹D. Yang, A. Ward, K. Halvorsen, and W. P. Wong, *Nat. Commun.* **7**, 11026 (2016).
- ⁴⁰R. McKendry, J. Zhang, Y. Arntz, T. Strunz, M. Hegner, H. P. Lang, M. K. Baller, U. Certa, E. Meyer, H.-J. Güntherodt, and C. Gerber, *Proc. Natl. Acad. Sci. U. S. A.* **99**, 9783 (2002).
- ⁴¹O. Guillaume-Gentil, E. Potthoff, D. Ossola, C. M. Franz, T. Zambelli, and J. A. Vorholt, *Trends Biotechnol.* **32**, 381 (2014).
- ⁴²K. C. Johnson, E. Clemmens, H. Mahmoud, R. Kirkpatrick, J. C. Vizcarra, and W. E. Thomas, *J. Biol. Eng.* **11**, 47 (2017).
- ⁴³N. Ribeck and O. A. Saleh, *Rev. Sci. Instrum.* **79**, 094301 (2008).
- ⁴⁴A. R. Bausch, W. Möller, and E. Sackmann, *Biophys. J.* **76**, 573 (1999).
- ⁴⁵D. O. Hebb, *The Organization of Behavior; a Neuropsychological Theory* (Wiley, Oxford, England, 1949).
- ⁴⁶J. D. Sweatt, *J. Neurochem.* **139**, 179 (2016).
- ⁴⁷E. L. Bienenstock, L. N. Cooper, and P. W. Munro, *J. Neurosci.* **2**, 32 (1982).
- ⁴⁸S. M. Dudek and M. F. Bear, *Proc. Natl. Acad. Sci. U. S. A.* **89**, 4363 (1992).
- ⁴⁹H.-K. Lee, K. Kameyama, R. L. Huganir, and M. F. Bear, *Neuron* **21**, 1151 (1998).
- ⁵⁰B. Gustafsson and H. Wigström, *J. Neurosci.* **6**, 1575 (1986).
- ⁵¹O. Paulsen and T. J. Sejnowski, *Curr. Opin. Neurobiol.* **10**, 172 (2000).
- ⁵²G. G. Turrigiano, K. R. Leslie, N. S. Desai, L. C. Rutherford, and S. B. Nelson, *Nature* **391**, 892 (1998).
- ⁵³D. Debanne, G. Daoudal, V. Sourdet, and M. Russier, *J. Physiol.* **97**, 403 (2003).
- ⁵⁴P. D. Maia and J. N. Kutz, *J. Comput. Neurosci.* **36**, 141 (2014).